Iraqi National Journal of Chemistry

Journal homepage:
http://iqnjc.com/Default.aspx

Development of a Sulfonated Magnetized Chitosan Biopolymer as a High-Performance Brønsted Acid Catalyst for the Synthesis of Tetrahydrobenzo[b]pyran

Ali Saad Obayes Al-Yasari

Islamic Azad University, Najaf Abad Branch, Faculty of Materials Engineering, Department of Chemistry, Iran

Abstract:

A magnetically recoverable Brønsted acid catalyst, Fe_3O_4@SiO_2-R-Chitosan-SO_3H, was synthesized via a four-step process involving chitosan activation, amination, immobilization onto Fe_3O_4@SiO_2, and sulfonation. FT-IR, XRD, and TGA-DTA analyses confirmed the formation of a stable organic–inorganic hybrid with preserved magnetic properties and a high density of strong acidic sites. The catalyst showed excellent performance in the ultrasound-assisted one-pot three-component synthesis of tetrahydrobenzo[b]pyran derivatives from malononitrile, dimedone, and aromatic aldehydes in ethanol. Under optimized conditions, yields of up to 94% were obtained within 1.5 h using only 0.05g of catalyst, with a TON of 11.1 and a TOF of 33.6 h-1. The catalyst exhibited broad substrate scope and maintained high activity over six consecutive cycles with minimal loss. The use of a green solvent, low catalyst loading, ultrasonic irradiation, and easy magnetic recovery underscores the sustainability and practical applicability of this catalytic system.

Keywords:

Multi-component reactions, Tetrahydrobenzo[b]pyran, Chitosan, Magnetic catalysts

1. Introduction

Multicomponent reactions (MCRs) are among the most efficient strategies in modern organic synthesis, enabling the one-pot combination of three or more reactants to rapidly generate structurally complex products with high atom economy. By minimizing waste, avoiding intermediate isolation, and shortening synthetic sequences, MCRs are particularly valuable for the rapid construction of heterocycles and small-molecule libraries relevant to medicinal chemistry. Ongoing advances, including the use of renewable feedstocks, low-energy activation methods, and computational or machine-learning tools for reaction prediction and optimization, continue to expand the scope and sustainability of MCR chemistry [1–5].

In parallel, magnetically recoverable nanocatalysts have emerged as powerful tools for sustainable synthesis. These systems combine the advantages of heterogeneous catalysis with facile magnetic separation, enabling efficient catalyst recovery and reuse without energy-intensive workup. Magnetic nanoparticles functionalized with acidic, basic, or metal-active sites have been successfully applied to a wide range of MCRs under mild and environmentally benign conditions, often in aqueous or solvent-free media [6-8].

Among heterocyclic scaffolds, pyran-annulated systems—particularly tetrahydrobenzopyrans-have attracted significant attention due to their structural diversity and broad biological relevance. These compounds exhibit diverse pharmacological activities, including anticancer, antimicrobial, antiviral, anti-inflammatory, and antioxidant properties, making them valuable targets in medicinal chemistry. Consequently, the development of efficient and green synthetic routes to tetrahydrobenzo[b]pyran derivatives remains an active area of research [9-15].

Traditionally, tetrahydrobenzo[b]pyrans are synthesized via a three-component condensation of dimedone, aldehydes, and active methylene compounds. Numerous catalytic systems—ranging from inorganic materials and sulfonated magnetic nanocomposites to carbon-based hybrids, supported ionic liquids, deep eutectic solvents, and bio-derived catalysts—have been explored to enhance efficiency and sustainability. These approaches typically proceed through tandem Knoevenagel-Michael cyclocondensation pathways and offer advantages such as high yields, low catalyst loading, operational simplicity, and catalyst recyclability under mild or solvent-free conditions [9-26].

Recent efforts increasingly integrate MCRs with heterogeneous and magnetic catalysis to further improve sustainability, substrate scope, and functional-group tolerance. Future developments are expected to emphasize green metrics, catalyst durability, and scalability through continuous or flow processes, positioning benzopyran synthesis at the intersection of medicinal relevance and sustainable chemistry [11-26]. Chitosan functionalization with sulfonic acid groups provides a solid Brønsted acid catalyst by immobilizing acidic sites on a renewable, biodegradable support. Incorporation of a magnetic core further enhances practicality by enabling rapid catalyst recovery, combining biobased sustainability with operational convenience [27-29].

In this work, we report the design and synthesis of a sulfonated magnetite-chitosan nanocomposite (Fe_3O_4@SiO_2-R-Chitosan-SO_3H) as a robust and recyclable Brønsted acid catalyst. Its catalytic performance was demonstrated in the one-pot, three-component synthesis of tetrahydrobenzo[b]pyran derivatives from aryl aldehydes, malononitrile, and dimedone (Scheme 1). This approach synergistically combines the efficiency of MCRs, the sustainability of a biopolymer-based catalyst, and the practicality of magnetic recovery, offering an effective strategy for green heterocyclic synthesis.

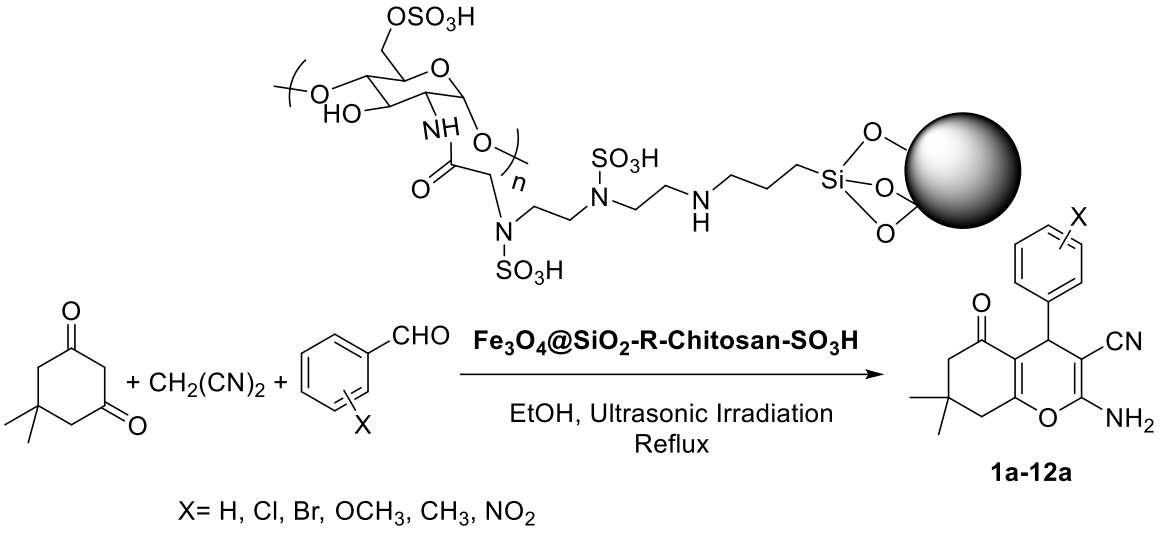

Scheme 1: Preparation of tetrahydrobenzo[b]pyran derivatives using Fe_3O_4@SiO_2-R-Chitosan-SO_3H

2. Experimental

2.1. Reagents and Instrumentation:

All chemicals used in this study were of analytical grade and applied without further purification. Chitosan (degree of deacetylation ≥95%, medium molecular weight), *N, N*-dimethylformamide (DMF, anhydrous, 99.8%), diethyl ether (≥99%), and acetone (≥99.5%) were obtained from Merck (Darmstadt, Germany). Aromatic aldehydes, malononitrile, and dimedone were also purchased from commercial suppliers and used as received.

Thermal stability of the samples was investigated by thermogravimetric and differential thermogravimetric analysis (TGA–DTG) using a Shimadzu TGA-DTG-60H analyzer under a nitrogen atmosphere with a heating rate of 10 °C min^{-1}. Fourier-transform infrared (FT-IR) spectra were recorded on a Bruker spectrophotometer using KBr pellets in the spectral range of 400–4000 cm^{-1}. Field-emission scanning electron microscopy (FE-SEM) images and elemental analyses were obtained using a JEOL JSM-IT100 microscope equipped with an energy-dispersive X-ray (EDX) detector. Ultrasonic reactions were performed in a digital ultrasonic bath operating at 40 kHz and 250 W. NMR spectra of the synthesized tetrahydrobenzo[b]pyran derivatives were recorded on a Bruker spectrometer operating at 500 MHz using DMSO-d_6 as the deuterated solvent, with chemical shifts (δ) reported in parts per million (ppm). Elemental (CHN) analyses were performed using a PerkinElmer 2400 Series II CHNS/O elemental analyzer to determine the carbon, hydrogen, and nitrogen contents of the synthesized materials.

2.2. Four Steps Preparation of Fe_3O_4@SiO_2-R-Chitosan-SO_3H

Step 1. Chitosan activation

Chitosan (5.0 g) was dispersed in anhydrous *N, N*-dimethylformamide (DMF, 150 mL) under a nitrogen atmosphere and cooled to 0°C using an ice bath. Chloroacetyl chloride (25 mL) was added dropwise over 30 min under continuous stirring. After completion of the addition, the reaction mixture was stirred at 0°C for 1h and then heated under reflux at 115°C for 3h. After cooling to room temperature, the resulting mixture was poured slowly into excess cold diethyl ether to precipitate the product. The solid was collected by filtration, washed thoroughly with

acetone to remove unreacted reagents, and vacuum-dried at 40°C to afford chloroacetylated chitosan as a pale solid.

Step 2. Amination

The obtained chloroacetylated chitosan was suspended in DMF (120 mL), and N^1-(2-aminoethyl)ethane-1,2-diamine (20 mL) was added dropwise under stirring. The reaction mixture was heated under reflux at 115 °C for 10 h. After completion, the mixture was cooled to room temperature and poured into excess cold acetone to precipitate the product. The solid was filtered, washed repeatedly with acetone and ethanol to remove excess diamine, and finally vacuum-dried at 40 °C to obtain amine-functionalized modified chitosan.

Step 3. Preparation of Fe_3O_4@SiO_2-R-Chitosan)

3-Chloropropyl triethoxysilane was bonded to Fe_3O_4@SiO_2 magnetic core according to the previously reported procedure [30]. The as-prepared nanoparticles (2.0 g) were dispersed in dry toluene (100 mL) by ultrasonication for 30 min. The modified chitosan (6.0 g) was then added to the suspension, followed by refluxing the mixture at 110°C for 24h under a nitrogen atmosphere. After cooling, the magnetized product was collected using an external magnet, washed successively with toluene, ethanol, and distilled water, and dried under vacuum at 50°C to give Fe_3O_4@SiO_2-R-Chitosan.

Step 4. Sulfonation of Magnetized Chitosan

The magnetized chitosan (1.5 g) was dispersed in dry toluene (100 mL) and cooled to 0°C. Chlorosulfonic acid ($ClSO_3H$, 3.0 mL) diluted in toluene (10 mL) was added dropwise over 20 min under stirring. The reaction mixture was then heated under reflux for 24h. After cooling to room temperature, the solid catalyst was magnetically separated and washed repeatedly with toluene, ethanol, and distilled water until a neutral pH was reached. Finally, the catalyst was vacuum-dried at 50°C to afford the final Fe_3O_4@SiO_2-R-Chitosan-SO_3H as a dark brown magnetic solid.

2.3. General Ultrasound-Assisted Procedure for the Synthesis of Tetrahydrobenzo[b]pyrans

In a typical experiment, malononitrile (1.0 mmol), dimedone (1.0 mmol), and the corresponding aromatic aldehyde (1.0 mmol) were added to a 50 mL round-bottom flask containing ethanol (25 mL) as a green solvent. Subsequently, Fe_3O_4@SiO_2-R-Chitosan-SO_3H (0.05 g) was introduced as a heterogeneous magnetic Brønsted acid catalyst. The reaction mixture was subjected to ultrasonic irradiation (40 kHz, 250 W) under reflux temperature and stirred continuously for the required reaction time (as listed in Table 2). The progress of the transformation was monitored by thin-layer chromatography (TLC). After completion, the reaction mixture was cooled to ambient temperature and the catalyst was rapidly separated using an external magnetic field. The crude product was dissolved in hot ethanol and purified by recrystallization to afford the corresponding tetrahydrobenzo[b]pyran derivatives in high purity and excellent yields. The recovered catalyst was washed with ethanol, dried under vacuum, and reused in subsequent runs.

Selected data:

2-amino-7,7-dimethyl-5-oxo-4-phenyl-5,6,7,8-tetrahydro-4H-chromene-3-carbonitrile (Table 2, Entry 1): ^{1}H-NMR (500 MHz, DMSO-d6): δ= 0.92 (s, 3H, CH_3), 1.02 (s, 3H, CH_3), 2.11-2.43(m,

4H), 4.18 (s, 1H), 6.87 (s, 2H, NH_2), 7.14 (t, *J* = 7.8 Hz, 2H), 7.29-7.34 (m, 3H) ppm. ^{13}C-NMR (125 MHz, DMSO-d_6): δ= 191.2, 161.9, 158.4, 144.1, 131.2, 129.3, 128.6, 120.2, 112.9, 57.8, 51.2, 35.7, 32.5, 28.9, 27.7 ppm. Elemental Analysis Found: C, 73.39; H, 6.18; N, 9.45; $C_{18}H_{18}N_2O_2$ Calculated: C, 73.45; H, 6.16; N, 9.52;

2-amino-7,7-dimethyl-5-oxo-4-(p-tolyl)-5,6,7,8-tetrahydro-4H-chromene-3-carbonitrile (Table 2, Entry 2): ^{1}H-NMR (500 MHz, DMSO-d6): δ= 0.93 (s, 3H, CH_3), 1.02 (s, 3H, CH_3), 2.10-2.41(m, 4H), 4.02 (s, 1H), 6.58 (s, 2H, NH_2), 7.03 (d, *J* = 7.8 Hz, 2H), 7.22 (d, *J* = 7.8 Hz, 2H) ppm. ^{13}C-NMR (125 MHz, DMSO-d_6): δ= 191.8, 162.0, 158.8, 144.3, 136.7, 129.2, 127.5, 126.6, 120.2, 112.7, 57.6, 51.2, 35.6, 32.5, 29.0, 27.6, 21.3 ppm. Elemental Analysis Found: C, 74.07; H, 6.59; N, 9.03; $C_{19}H_{20}N_2O_2$ Calculated: C, 74.00; H, 6.54; N, 9.08.

3. Results and discussion

3.1. Catalyst Schematic preparation and characterization

The magnetically separable solid acid catalyst, Fe_3O_4@SiO_2-R-Chitosan-SO_3H, was synthesized through a multi-step procedure to integrate distinct functionalities (Scheme 2). A core of superparamagnetic Fe_3O_4 nanoparticles was first encapsulated within an inert silica shell to ensure chemical stability. This Fe_3O_4@SiO_2 intermediate was then silanized to provide reactive sites for the covalent immobilization of a chitosan polymer network. Subsequent sulfonation of the grafted chitosan introduced strong Brønsted acid sites, resulting in a composite catalyst designed for efficient use in acid-promoted reactions and straightforward recovery via magnetic separation. The synthesis of Fe_3O_4@SiO_2-R-Chitosan-SO_3H is a masterclass in nanomaterial design, where each component is engineered to address a specific challenge. The Fe_3O_4 core provides magnetic separability, the SiO_2 shell ensures chemical robustness, the chitosan matrix offers a versatile and green platform, and the SO_3H groups impart potent catalytic function. This synergistic integration results in a high-performance, magnetically recoverable catalyst that aligns perfectly with the principles of Green Chemistry. It minimizes waste, energy, and resource use through its reusability and by leveraging a renewable biopolymer, thereby presenting a sustainable and efficient solution for modern chemical synthesis.

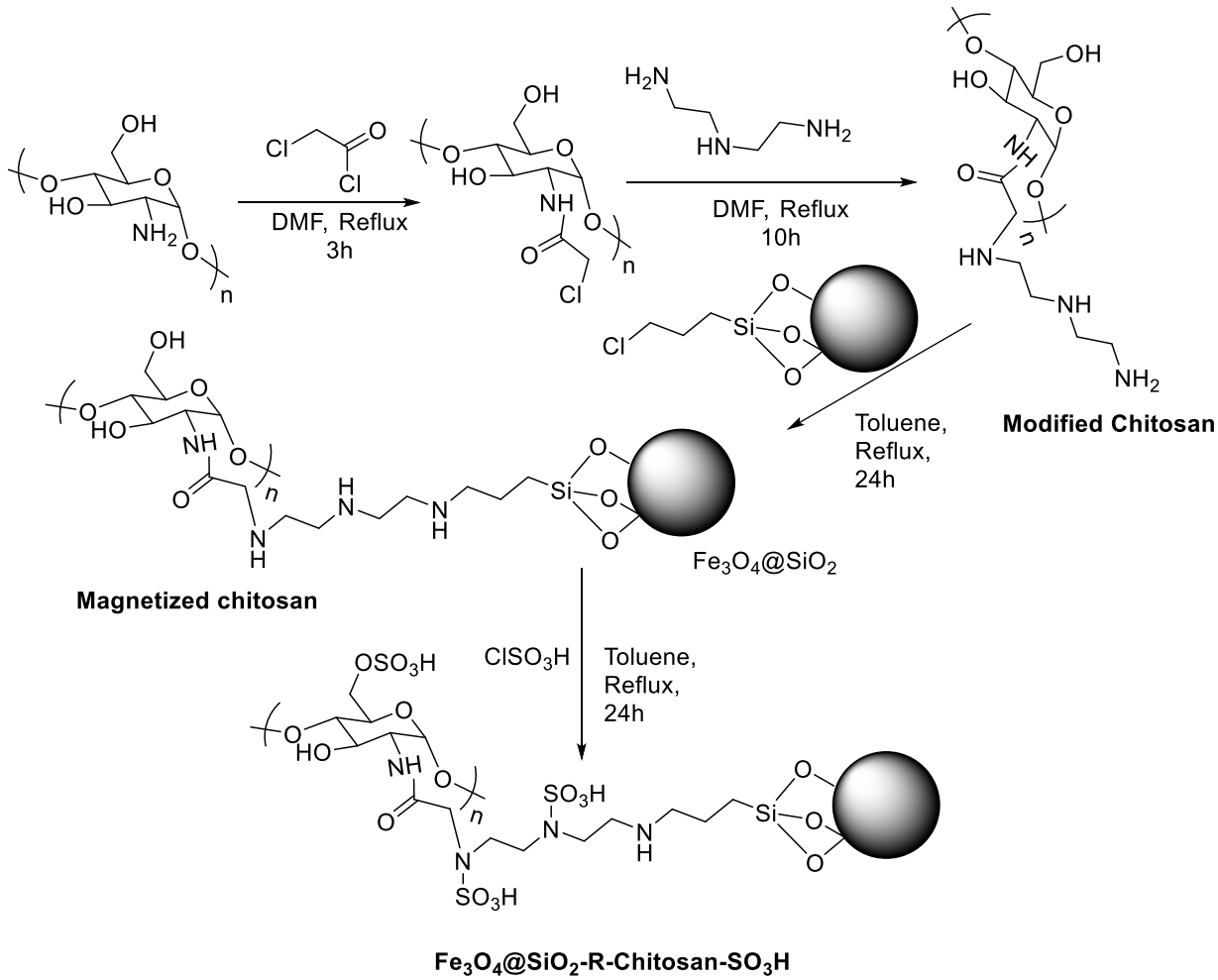

Scheme 2: Schematic preparation of the Fe_3O_4@SiO_2-R-Chitosan-SO_3H

The FT-IR spectrum of the Fe_3O_4@SiO_2-R-Chitosan-SO_3H composite (Figure 1) confirms the successful integration of all structural components. The broad band at 3200-3700 cm^{-1} arises from overlapping O-H and SO_3H stretching vibrations from chitosan, silica surface hydroxyls, and sulfonic acid groups. The weak band near 2920 cm^{-1} corresponds to aliphatic C–H stretching. Absorptions at 1675 and 1723 cm^{-1} are attributed to amide C=O and O-C-O vibrations of chitosan, while bands at 1088, 1185, and 1278 cm^{-1} originate from C-C, C-O, and C-N stretching. The band at 1423 cm^{-1} (SO_2 vibration) confirms sulfonation. Strong Si-O-Si stretching at 1030-1090 cm^{-1} verifies silica shell formation, and the Fe-O vibration at 450-600 cm^{-1} confirms retention of the magnetite core, collectively validating the formation of the hybrid composite.

The XRD pattern of Fe_3O_4@SiO_2-R-Chitosan-SO_3H (Figure 1) shows distinct reflections at 36.3, 42.3, 52.7, 56.8, and 61.8 [2θ°], consistent with the cubic spinel structure of Fe_3O_4 (PDF 00-003-0862), indicating preservation of the magnetic core after coating and functionalization. The broad halo between 15-30° is attributed to amorphous SiO_2 and disordered chitosan, while the weak feature at 45-50° reflects disrupted semicrystalline domains of modified chitosan. The coexistence of crystalline Fe_3O_4 peaks and amorphous halos confirms the formation of a core–shell hybrid structure suitable for catalytic applications.

TGA-DTA analysis reveals a multistep thermal decomposition profile characteristic of the hybrid nanocomposite. The initial weight loss below 200 °C corresponds to desorption of physically adsorbed water. An exothermic event at 250-330 °C is associated with the decomposition of

sulfonic acid groups, while the major degradation step between 330-500 °C arises from chitosan backbone breakdown, with the shifted onset indicating enhanced thermal stability due to crosslinking (Figure 1). The remaining residue corresponds to the stable Fe_3O_4@SiO_2 core, enabling estimation of organic content. These results confirm the layered architecture and demonstrate thermal stability under moderately elevated temperatures.

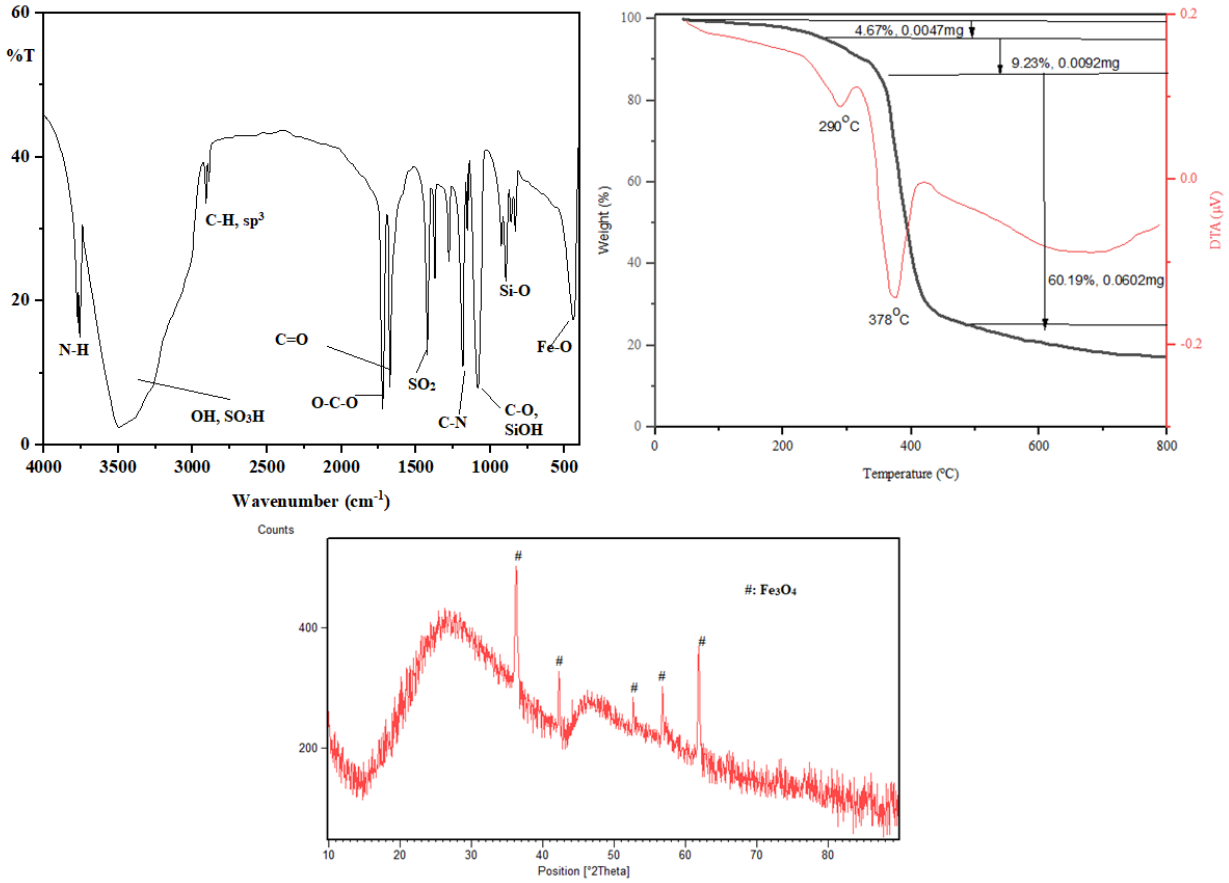

Figure 1: FT-IR, TGA-DTA, and XRD analysis of Fe_3O_4@SiO_2-R-Chitosan-SO_3H polymeric systems

3.2. Catalyst potential Fe_3O_4@SiO_2-R-Chitosan-SO_3H investigation

Next, Fe_3O_4@SiO_2-R-Chitosan-SO_3H, a new magnetically recoverable catalyst, was used for the three-component synthesis of tetrahydrobenzo[b]pyrans. At the start of the catalytic experiments to evaluate the catalytic potential of Fe_3O_4@SiO_2-R-Chitosan-SO_3H, the condensation of dimedone, benzaldehyde, and malononitrile was used as a model reaction. The reaction conditions were systematically optimized by screening various catalysts, solvents, and catalyst loadings, with the results summarized in Table 1. Initially, several homogeneous and heterogeneous Brønsted acids were evaluated for the model reaction under ultrasonic irradiation in refluxing ethanol. Homogeneous catalysts such as H_2SO_4 and $HClO_4$ proved inefficient, yielding 34% and 25% of the product, respectively, while CH_3COOH yielded no product (Entries 1-3). Among the solid acids, SiO_2-SO_3H and SiO_2-$HClO_4$ provided improved yields of 85% and 64% (Entries 4-5).

However, Fe_3O_4@SiO_2-R-Chitosan-SO_3H demonstrated superior catalytic performance, achieving an excellent 94% yield in just 1.5 hours (Entry 6).

Subsequently, the influence of the reaction medium was investigated using the optimal catalyst, Fe_3O_4@SiO_2-R-Chitosan-SO_3H. Polar aprotic solvents like CH_3CN and toluene afforded moderate yields (55% and 41%, respectively), while Et_2O, hexane, and EtOAc were entirely ineffective (Entries 7-12). Notably, the reaction proceeded poorly in water (32% yield) and under solvent-free conditions at 100 °C (52% yield), confirming that refluxing ethanol is the optimal solvent for this catalytic system (Entries 10, 13). Finally, the effect of catalyst loading was examined. A reduced loading of 0.01 g yielded 20% over 3 hours (Entry 14). Increasing the loading to 0.025 g improved the yield to 68% in 2 hours (Entry 15). The optimal balance of reaction time and efficiency was achieved with 0.05 g of catalyst, yielding 94% in 1.5 hours (Entry 6). While a further increase to 0.075 g slightly shortened the reaction time to 1.2 hours, the yield was comparable (92%, Entry 16), and a 0.1 g loading led to a marginally lower yield of 89% in 1 hour (Entry 17). Therefore, 0.05 g of Fe_3O_4@SiO_2-R-Chitosan-SO_3H in refluxing ethanol under ultrasonic irradiation was established as the optimal protocol, offering an outstanding combination of high yield and short reaction time.

Consequently, under the optimal conditions obtained, the scope of this method was expanded, and a series of substituted aldehydes was converted into the desired products in good to excellent yields (Table 2). As shown in Table 2, the reaction of dimedone, various aldehydes, and malononitrile proceeded effectively to afford the products in high yields.

Table 1: Optimization of the reaction condition			
Entry	Catalyst	Condition	Time (h) / Yield (%)*
1	H_2SO_4 (1mmol)	EtOH, Ultrasonic Irradiation, Reflux	2/34
2	CH_3COOH (1mmol)	EtOH, Ultrasonic Irradiation, Reflux	2/-
3	$HClO_4$ (1mmol)	EtOH, Ultrasonic Irradiation, Reflux	2/25
4	SiO_2-SO_3H (0.05g, 0.5mmol H^+)	EtOH, Ultrasonic Irradiation, Reflux	2/85
5	SiO_2-$HClO_4$ (0.05g, 0.5mmol H^+)	EtOH, Ultrasonic Irradiation, Reflux	2/64
6	Fe_3O_4@SiO_2-R-Chitosan-SO_3H (0.05g, 0.62mmol H^+)	EtOH, Ultrasonic Irradiation, Reflux	1.5/94
7	Fe_3O_4@SiO_2-R-Chitosan-SO_3H (0.05g, 0.62mmol H^+)	Et_2O, Ultrasonic Irradiation, Reflux	5/-
8	Fe_3O_4@SiO_2-R-Chitosan-SO_3H (0.05g, 0.62mmol H^+)	CH_3CN, Ultrasonic Irradiation, Reflux	2/55
9	Fe_3O_4@SiO_2-R-Chitosan-SO_3H (0.05g, 0.62mmol H^+)	Toluene, Ultrasonic Irradiation, Reflux	2/41
10	Fe_3O_4@SiO_2-R-Chitosan-SO_3H (0.05g, 0.62mmol H^+)	H_2O, Ultrasonic Irradiation, Reflux	2/32
11	Fe_3O_4@SiO_2-R-Chitosan-SO_3H (0.05g, 0.62mmol H^+)	Hexane, Ultrasonic Irradiation, Reflux	5/-
12	Fe_3O_4@SiO_2-R-Chitosan-SO_3H (0.05g, 0.62mmol H^+)	EtOAc, Ultrasonic Irradiation, Reflux	3/-
13	Fe_3O_4@SiO_2-R-Chitosan-SO_3H (0.05g, 0.62mmol H^+)	solvent-free, 100 °C	1.5/52
14	Fe_3O_4@SiO_2-R-Chitosan-SO_3H (0.01g, 0.16mmol H^+)	EtOH, Ultrasonic Irradiation, Reflux	3/20
15	Fe_3O_4@SiO_2-R-Chitosan-SO_3H (0.025g, 0.31mmol H^+)	EtOH, Ultrasonic Irradiation, Reflux	2/68
16	Fe_3O_4@SiO_2-R-Chitosan-SO_3H (0.075g, 0.93mmol H^+)	EtOH, Ultrasonic Irradiation, Reflux	1.2/92
17	Fe_3O_4@SiO_2-R-Chitosan-SO_3H (0.1g, 1.12 mmol H^+)	EtOH, Ultrasonic Irradiation, Reflux	1/89
*Isolated Yield;			

Overall, aromatic aldehydes with electron-donating groups showed lower reactivity than those with electron-withdrawing groups. Furthermore, aldehydes substituted at the *ortho* position reacted more slowly compared to those at the *para* position. These results indicate that the electronic nature of the substituent groups has a little significant influence on the reaction yields (Table 2). Heterocyclic aldehydes such as thiophene-2-carbaldehyde also afforded good results in a short time.

The role the catalyst can be explained using a plausible mechanism. Scheme 3 shows the proposed mechanism for the synthesis of tetrahydrobenzo[b]pyran derivatives. According to published literature, the first step is a Knoevenagel condensation, which can be followed by a

Michael addition, forming an intermediate. This intermediate then undergoes cyclization which produces the desired product.

Table 2: Preparation of tetrahydrobenzo[b]pyrans. using Fe_3O_4@SiO_2-R-Chitosan-SO_3H,

Entry	Aldehyde	Product	Time (h)	Yield (%)	M.p. (°C) [Ref.]
1	Benzaldehyde	1a	1.5	94	231-233 [232-234][9]
2	4-Methyl benzaldehyde	2a	3	90	219-221 [218-219][31]
3	4-Methoxy benzaldehyde	3a	4	88	200-202 [197-199][31]
4	4-Nitro benzaldehyde	4a	1	92	175-177 [178-180][31]
5	3-Nitro benzaldehyde	5a	1	95	215-217 [212-214][31]
6	3-Chloro benzaldehyde	6a	1.3	96	225-227 [225-226][31]
7	4-Chloro benzaldehyde	7a	1.2	94	216-218 [214-216][9]
8	4-Bromo benzaldehyde	8a	1.1	95	207-209 [204-206][9]
9	2,4-diChloro benzaldehyde	9a	1.5	91	221-223[218-220][20]
10	2-Chloro benzaldehyde	10a	2	96	205-207 [200-202][31]
11	3,4-diChloro benzaldehyde	11a	1	97	225-227[-]
12	Thiophene-2-carboxaldehyde	12a	2	85	216-218 [212-214][18]

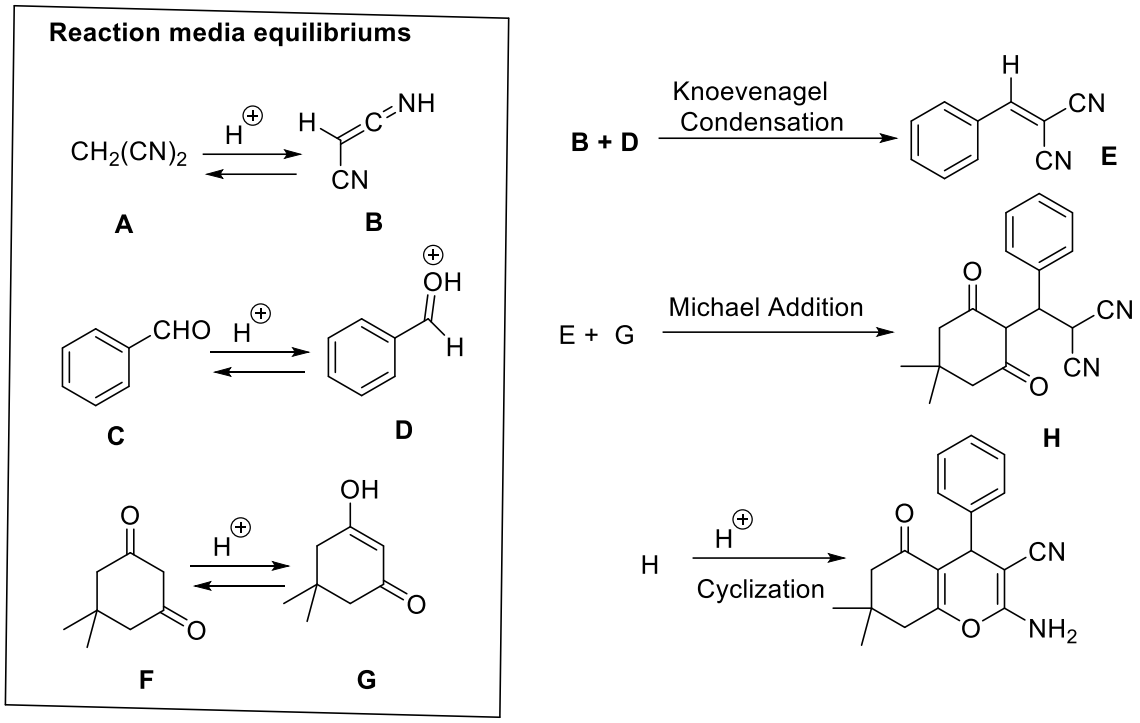

Scheme 3: Proposed mechanism for the synthesis of tetrahydrobenzo[b]pyrans

Finally, the catalyst was recovered by simple magnetic filtration and, after washing with ethanol, was reused for subsequent reactions. The catalyst was used seven times in subsequent reactions without a significant loss of catalytic activity (Figure 4).

Furthermore, it is remarkable to note that the condensation proceeds with a slight amount of Fe_3O_4@SiO_2-R-Chitosan-SO_3H concentration and gives tetrahydrobenzo[b]pyrans in good yields. Interestingly, the heterogeneous Fe_3O_4@SiO_2-R-Chitosan-SO_3H was not deactivated and could be reused several times. Seven consecutive runs of the reaction of dimedone, benzaldehyde, and malononitrile with Fe_3O_4@SiO_2-R-Chitosan-SO_3H were carried out (Figure 2). The results demonstrate that there is almost no significant change in the activity of Fe_3O_4@SiO_2-R-Chitosan-SO_3H, so it can be used at least 5 times successfully, leading to high turnover numbers (TONs). The catalyst exhibited high intrinsic activity with a TON of 11.1 and TOF of 33.6 h^{-1}, and could be recycled for six consecutive runs with only a minor decrease in yield, confirming its excellent stability. The use of a green solvent, low catalyst loading, energy-efficient ultrasound assistance, and easy magnetic recovery collectively highlight the sustainability and practical applicability of this catalytic system.

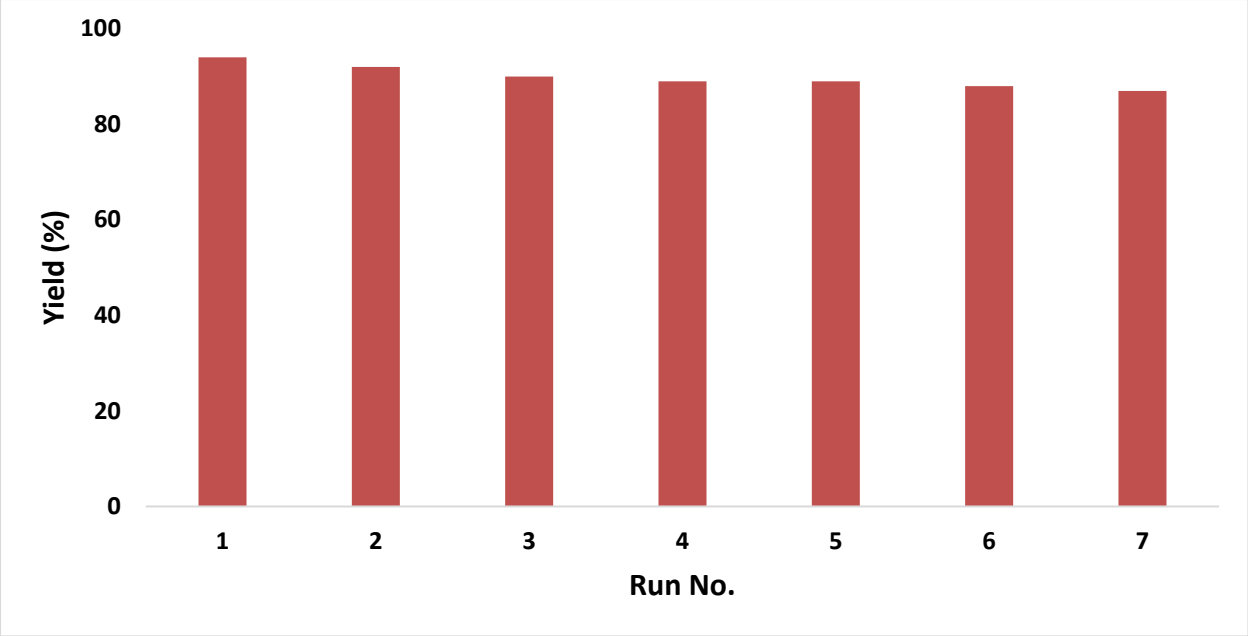

Figure 2: Catalyst recycling results

4. Conclusions

In this work, an efficient and environmentally benign magnetic Brønsted acid catalyst, Fe_3O_4@SiO_2-R-Chitosan-SO_3H, was successfully designed and applied for the ultrasound-assisted synthesis of tetrahydrobenzo[b]pyran derivatives. The catalyst demonstrated excellent structural stability, high catalytic activity, and strong recyclability due to the synergistic integration of a magnetic core, a protective silica shell, a renewable chitosan framework, and highly active sulfonic acid groups. Under optimized conditions, a wide range of aromatic aldehydes was converted into the desired products in high to excellent yields within short reaction times. The catalyst retained its activity over multiple reuse cycles and showed high TON and TOF values, confirming its efficiency and durability. The use of ethanol as a green solvent, low catalyst loading, ultrasonic energy assistance, and simple magnetic separation collectively make this protocol an attractive, sustainable, and scalable approach for the synthesis of biologically important heterocyclic compounds.

Acknowledgments

The laboratory support by the University of Islamic Azad University, Najaf Abad Branch, Faculty of Materials Engineering, Department of Chemistry, Iran, is highly acknowledged.

Declarations

Ethical Approval

Not applicable

Competing interests

The authors declare that they have no interests that could influence the work reported in this paper.

Funding

No funding was received for conducting this study.

Availability of data and materials

The data supporting our findings are available in the text of this article.

References

[1] K. Venkatesan, M. E. A. Zaki, S.-K. Chang, L. S. Wong, and S. M. Gomha, "Enzyme-catalysed multicomponent reactions (MCRs) for the green synthesis of bioactive heterocycles: A review," *Results in Chemistry*, vol. 18, p. 102835, 2025, doi: 10.1016/j.rechem.2025.102835.

[2] M. Abushuhel, R. Ali, S. Ganesan, S. Al-Hasnaawei, M. Kazemi, K. Jayabalan, R. Sharma, and A. Sinha, "Magnetic carbon nanotubes in multicomponent reactions: A path to sustainable heterocyclic synthesis," *Journal of Organometallic Chemistry*, p. 123971, 2025, doi: 10.1016/j.jorganchem.2025.123971.

[3] H. Yazdani, S. E. Hooshmand, and A. Al-Harrasi, "Ball-milling multicomponent reactions for diverse organic transformations," *Tetrahedron*, vol. 185, p. 134863, 2025, doi: 10.1016/j.tet.2025.134863.

[4] T. Ahmadi, G. M. Ziarani, P. Gholamzadeh, and H. Mollabagher, "Recent advances in asymmetric multicomponent reactions (AMCRs)," *Tetrahedron: Asymmetry*, vol. 28, no. 5, pp. 708–724, 2017, doi: 10.1016/j.tetasy.2017.04.002.

[5] L. H. Choudhury and T. Parvin, "Recent advances in the chemistry of imine-based multicomponent reactions (MCRs)," *Tetrahedron*, vol. 67, no. 43, pp. 8213–8228, 2011, doi: 10.1016/j.tet.2011.07.020.

[6] P. Kumar, V. Tomar, D. Kumar, R. K. Joshi, and M. Nemiwal, "Magnetically active iron oxide nanoparticles for catalysis of organic transformations: A review," *Tetrahedron*, vols. 106–107, p. 132641, 2022, doi: 10.1016/j.tet.2022.132641.

[7] Vaishali, S. Sharma, K. Bhatrola, A. Irfan, N. Devi, K. Mishra, K. Dubey, A. Mittal, E. Mateev, and V. K. Vashistha, "Green synthesis of imidazoles: The catalytic efficacy of magnetic nanoparticles," *Tetrahedron*, vol. 167, p. 134246, 2024, doi: 10.1016/j.tet.2024.134246.

[8] R. Perumal, B. Bathrinarayanan, M. Ghashang, and S. S. Mansoor, "An efficient one-pot synthesis of 7,7-dimethyl-2-(2-oxo-2H-chromen-3-yl)-4-aryl-7,8-dihydroquinolin-5(6H)-one derivatives using chitosan-SO_3H as a biodegradable organocatalyst," *Journal of Heterocyclic Chemistry*, vol. 56, no. 3, pp. 947–955, 2019.

[9] S. Sibous *et al.*, "Apatite tricalcium phosphate powder $Ca_9(HPO_4)(PO_4)_5(OH)$ as an effective and eco-friendly catalyst for the green synthesis of 3,4-dihydropyrano[c]chromenes and tetrahydrobenzo[b]pyrans derivatives," *Polyhedron*, vol. 277, p. 117565, 2025, doi: 10.1016/j.poly.2025.117565.

[10] R. Shekhanavar, S. Khatavi, and K. Kamanna, "Eco-friendly one-pot synthesis of tetrahydrobenzo[b]pyran and dihydropyrano[3,2-c]chromene derivatives using functionalized Fe_3O_4@SiO_2@SO_3H under microwave irradiation," *Polycyclic Aromatic Compounds*, vol. 45, no. 1, pp. 60–79, 2025, doi: 10.1080/10406638.2024.2389939.

[11] F. Ataie, A. Davoodnia, and A. Khojastehnezhad, "Graphene oxide functionalized organic–inorganic hybrid (GO–Si–NH_2-PMo): An efficient and green catalyst for the synthesis of tetrahydrobenzo[b]pyran derivatives," *Polycyclic Aromatic Compounds*, vol. 41, no. 4, pp. 781–794, 2021.

[12] H. R. Saadati-Moshtaghin and F. Abbasinohoji, "$LaMnO_3$ supported ionic liquid as an efficient catalyst for one-pot synthesis of tetrahydrobenzo[b]pyran derivatives under solvent-free conditions," *Polycyclic Aromatic Compounds*, vol. 41, no. 3, pp. 455–466, 2021.

[13] M. Biglari, F. Shirini, N. O. Mahmoodi, M. Zabihzadeh, and M. Mashhadinezhad, "Deep eutectic solvent promoted three-component synthesis of tetrahydrobenzo[b]pyran derivatives," *Journal of Molecular Structure*, vol. 1205, p. 127652, 2020.

[14] F. Shirini, M. Safarpoor Nikoo Langarudi, and N. Daneshvar, "Preparation of a new DABCO-based ionic liquid and its application in tetrahydrobenzo[b]pyran synthesis," *Journal of Molecular Liquids*, vol. 234, pp. 268–278, 2017.

[15] F. Pirani and H. Eshghi, "Design and application of a natural deep eutectic solvent for the synthesis of tetrahydrobenzo[b]pyrans," *Heliyon*, vol. 11, no. 16, p. e44094, 2025.

[16] S. S. Pourpanah, S. M. Habibi-Khorassani, and M. Shahraki, "Fructose-catalyzed synthesis of tetrahydrobenzo[b]pyran derivatives," *Chinese Journal of Catalysis*, vol. 36, no. 5, pp. 757–763, 2015.

[17] S. F. Hojati, N. MoeiniEghbali, S. Mohamadi, and T. Ghorbani, "Trichloroisocyanuric acid as an efficient catalyst for tetrahydrobenzo[b]pyran synthesis," *Organic Preparations and Procedures International*, vol. 50, no. 4, pp. 408–415, 2018.

[18] N. Hazeri *et al.*, "Starch solution as a catalyst for one-pot synthesis of tetrahydrobenzo[b]pyrans," *Chinese Journal of Catalysis*, vol. 35, no. 3, pp. 391–395, 2014.

[19] M. A. Zolfigol, M. Yarie, and S. Baghery, "Nanostructured molten salt catalyst for tetrahydrobenzo[b]pyran synthesis," *Journal of Molecular Liquids*, vol. 222, pp. 923–932, 2016.

[20] M. A. Zolfigol *et al.*, "Reusable molten salt catalyst for tetrahydrobenzo[b]pyrans via Knoevenagel–Michael cyclocondensation," *Journal of Molecular Liquids*, vol. 221, pp. 851–859, 2016.

[21] F. Adibian *et al.*, "Nanocomposite catalyst based on functionalized carbon nanotubes for tetrahydrobenzo[b]pyran synthesis," *Polyhedron*, vol. 175, p. 114179, 2020.

[22] D. Azarifar and Y. Abbasi, "Sulfonic acid–functionalized magnetic $Fe_{3-x}Ti_xO_4$ nanoparticles as recyclable catalysts," *Synthetic Communications*, vol. 46, no. 9, pp. 745–758, 2016.

[23] B. Mashhourzad and B. Zeynizadeh, "Magnetically recoverable Fe_3O_4@chitosan@Ni_2B as a bio-based catalyst," *Nanoscale Advances*, vol. 7, no. 12, pp. 3701–3721, 2025.

[24] D. Azarifar, O. Badalkhani, and Y. Abbasi, "Silica-modified magnetite grafted with sulfamic acid groups," *Journal of Sulfur Chemistry*, vol. 37, no. 6, pp. 656–673, 2016.

[25] S. Rathod, B. Arbad, and M. Lande, "Nanosized $CeMg_xZr_{1-x}O_2$ catalyst for tetrahydrobenzo[b]pyran synthesis," *Chinese Journal of Catalysis*, vol. 31, no. 6, pp. 631–636, 2010.

[26] M. Behboudi Laeen and A. R. Pourali, "Magnetic immobilized ionic liquid for three-component synthesis of tetrahydrobenzo[b]pyrans," *Current Organocatalysis*, vol. 12, no. 2, pp. 83–94, 2025.

[27] I. Souza de Jesus *et al.*, "Recent advances in sulfonic acid chitosan as heterogeneous organocatalyst," *Current Organic Chemistry*, vol. 29, no. 14, pp. 1078–1091, 2025.

[28] S. Darvishi, S. Sadjadi, and M. M. Heravi, "Sulfonic acid-functionalized chitosan–MOF composite for fructose conversion," *Scientific Reports*, vol. 14, p. 5834, 2024.

[29] I. S. de Jesus *et al.*, "Direct lawsone O-alkylation using sulfonic acid-functionalized chitosan," *ACS Omega*, vol. 10, no. 4, pp. 4163–4169, 2025.

[30] M. Khalaj, S. M. Musavi, and M. Ghashang, "Alkyl ammonium hydrogen sulfate immobilized on Fe_3O_4@SiO_2 nanoparticles," *Scientific Reports*, vol. 14, p. 8870, 2024.

[31] P. Patil, S. Kadam, D. Patil, and P. More, "Metal- and halide-free ionic liquid catalyzed synthesis of tetrahydrobenzo[b]pyrans," *Journal of Molecular Liquids*, vol. 345, p. 117867, 2022.